

Noise Analysis and Optical Design of an Optical Fiber Seismometer with a Super-Long Refraction Arm

B. Wu, J. Yang*, Y. G. Yuan, J. G. You, F. Peng, and L. B. Yuan

Photonics Research Center, School of Science, Harbin Engineering University, Harbin 150001, P. R. China

(Received: 16 July 2011. Accepted: 22 October 2011)

In this paper, we proposed an fiber seismometer based on a fiber-optic interferometer with a super-long arm to detect seismic waves. The interferometer was composed of a sensing fiber which was wrapped between two measurement points, and a reference fiber which was completely isolated from the vibration. The seismic signal could be obtained by directly detecting the strain and vibration between two measurement points fixed on rocks without an inertial pendulum. The strain and vibration were amplified due to the multi-layer wrapped sensing fiber. We studied the optical structure and parameter design of the fiber seismometer, analyzed the effect of thermal noise, Rayleigh noise and shot noise, and optimized the sensitivity and resolution. The experimental results indicated that the measurement resolution of the seismometer with the interference arm length of 1000 m was higher than $100 \text{ pm/Hz}^{1/2}$.

Keywords: Fiber Seismometer, Sensitivity Enhancement, Noise Analysis, Optical Design.

1. INTRODUCTION

In recent years, geological activities become active and strong earthquakes have occurred around the world, which results in heavy casualties and economic losses. For example, the $M = 8.0$ Wenchuan earthquake of China in 2008 and the $M = 9.0$ earthquake of Japan in 2011, both caused tens of thousands of casualties, in particularly, the Indian Ocean tsunami resulted from the strong earthquake caused hundreds of thousands of casualties. The earthquakes made grave destructions to human activities, so the research on the earthquakes attracts wide attention.

The most effective method to study on earthquake is detecting seismic waves, so we can know the law of geological activities. Compared to the traditional electromechanical seismometer, there is no electronic circuit in the sensing element of fiber seismometers, which means that the thermal noise can be greatly decreased, and the potential noise level will be significantly lower than the Peterson low noise model.¹ The optical seismic monitoring technique has advantages such as high sensitivity, anti-electromagnetic interference, corrosion resistance, large dynamic range and broad frequency bandwidth. Recently, various types of fiber-optic sensors based on intensity modulation,² phase

modulation³ and polarization modulation⁴ have been developed to detect seismic waves.

In this paper, we developed a fiber seismometer based on Michelson interferometer. Without employing an inertia pendulum, the seismometer can directly detect the strain and vibration between two rocks. The vibration signal was amplified by the multi-turn wrapped sensing fiber, so that we can detect the weak crustal deformation and seismic waves.

2. THE MEASUREMENT PRINCIPLE OF A FIBER SEISMOMETER

The fiber seismometer is based on Michelson interferometry, as shown in Figure 1. The interference arms are wrapped several circles around two cylinders which fixed on the rocks, which can amplify vibration signal. The light intensity detected by the photodetector is given by

$$I = A_1^2 + A_2^2 + 2A_1A_2 \cos(2\pi\Delta L/\lambda_{LS}) \quad (1)$$

where A_1 and A_2 are the amplitudes of the sensing and reference arms respectively, ΔL is the optical path difference between the two arms, λ_{LS} is the center wavelength of the laser.

If the distance between the two rocks changes Δl , the optical path difference between the sensing arm and the

*Corresponding author; Email: yangjun141@263.net

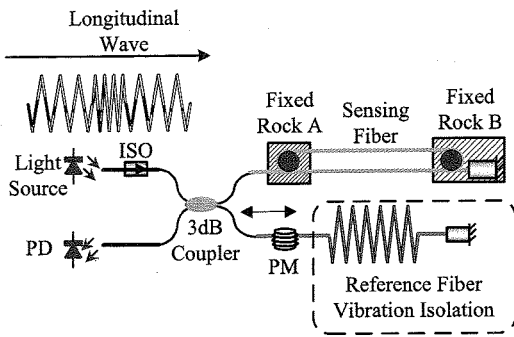


Fig. 1. Fiber optic seismometer.

reference arm will change to be $\Delta L + 2n\Delta l$. Then the light intensity received by the photodetector is

$$I = I_0(1 + \gamma \cos k(\Delta L + 2n\Delta l)) \quad (2)$$

where $k = 2\pi/\lambda_{LS}$, n is the medium refractive index of the fiber, $\gamma = 2(A_1/A_2)/[1 + (A_1/A_2)^2]$ is the contrast ratio of the interference signal.

If a longitudinal seismic wave acts on rocks A and B at time t , the vibrations of the rocks can be identified as:

$$\begin{cases} x_A = A_m \cos(\omega_{SW}t + \varphi) \\ x_B = A_m \cos(\omega_{SW}t + \Delta\varphi + \varphi) \end{cases} \quad (3)$$

where A_m is the amplitude of the rock's vibration caused by the seismic wave, ω_{SW} is the angular frequency, φ is the initial phase. The distance between the rocks is L , the velocity of the seismic wave is ν_{SW} , the phase difference of seismic wave between A and B caused from the seismic waves is $\Delta\varphi$, which is written as

$$\Delta\varphi = -\frac{2\pi L}{\lambda_{SW}} \quad (4)$$

where λ_{SW} is the wavelength of seismic waves. Then the phase difference of the interferometer is

$$\Delta\phi = \frac{4\pi n A_m}{\lambda_{LS}} \sin\left[\frac{\pi L}{\lambda_{SW}}\right] \sin\left[\omega_{SW}t - \frac{\pi L}{\lambda_{SW}} + \varphi\right] \quad (5)$$

According to Eq. (5), when $L/\nu_{SW} < t$, the interferometer response is equal to the vibration frequency of rock A. The propagation law of the vibration wave are invariant while the phase change is $\pi L/\lambda_{SW}$, therefore the ratio of the present amplitude to the original one is $(4\pi n A_m/\lambda_{LS}) \sin[\pi L/\lambda_{SW}]$. The response of the interferometer corresponds to the ratio of the interferometer arm length L to the seismic wavelength λ_{SW} . The responsibility reaches to its maximum $(4\pi n A_m/\lambda_{LS})$ when $2L/\lambda_{SW}$ is odd, and to its minimum (zero) when $2L/\lambda_{SW}$ is even. The maximum detectable frequency of seismic is designed to be 1 kHz, and velocity of seismic waves propagating in granites is 3950 m/s. Therefore, based on the actual situation, the distance between rocks of the fiber seismometer is set to 2 m.

3. THE NOISE ANALYSIS OF THE FIBER SEISMOMETER

3.1. The Analysis of Rayleigh Noise

Because the source used in the fiber seismometer is a narrow linewidth laser, Rayleigh scattering becomes one of the main noise sources. Assume that the fiber loss α_R is mainly caused by Rayleigh noise, the intensity of the backscatter along the fiber can be expressed as⁵

$$I_{bs} = I_0(1 - 10^{-\alpha_R L/10})S \quad (6)$$

The ratio of the backscatter intensity to the total backscatter intensity from all directions is called recovery factor S , which is approximately equal to the ratio of the fiber solid acceptance angle to the full solid angle with the steradian of 4π , typically, $S \approx 10^{-3}$.

As described by Lloyd et al.⁶ the maximum phase noise caused by Rayleigh scatter is given by

$$\phi_n \approx 2\sqrt{\alpha_b L} \quad (7)$$

where L is the length of the fiber ring, $\alpha_b = \alpha_R S$ is the backscatter coefficient of the light. In Ref. [6] the backscatter phase noise is $12 \mu\text{rad}/\sqrt{\text{Hz}}$ for a 235 m long fiber ring. Substituting these numbers into Eq. (7), we can get the maximum backscatter noise of the Michelson interferometer with 1000 m long arms:

$$\phi_{MR} = \frac{12}{\sqrt{235/2000}} \approx 35 \mu\text{rad}/\sqrt{\text{Hz}} \quad (8)$$

If the center wavelength of the Michelson interferometer is 1550 nm, the equivalent measurement displacement of the demodulated phases is equal to

$$\frac{L_{\min}}{\phi_{MR}} = \frac{\lambda}{2} \cdot \frac{1}{2\pi} \quad (9)$$

Under the influence of maximum backscatter noise, the resolution limit of measurement displacement is approximately $4.3 \text{ pm}/\text{Hz}^{1/2}$.

3.2. The Optimization of the Fiber Length

Typically, the measurement limit of the sensor is built on the noise limit of the fiber interferometer. The intrinsic thermal noise existing in the fiber and the sensing probe is the base noise limit of the sensing system. The intrinsic thermal noise can be approximately given by,⁷⁻⁸

$$\Delta\phi_{\text{temp}} \text{ (dB)} = [-147 + 10 \log(L)] \text{ dB}(\text{rad}/\text{Hz}^{1/2}) \quad (10)$$

The thermal noise of the fiber decreases as the frequency increases. With the length of the reference arm and the sensing arm both 1000 m (the total length of the fiber is 2000 m), the minimum noises are about $3.3 \mu\text{rad}/\sqrt{\text{Hz}}@1 \text{ kHz}$ and $100 \mu\text{rad}/\sqrt{\text{Hz}}@1 \text{ Hz}$.

Shot noise caused from the dispersion of carriers is another kind of noise, and it can be written as

$$\Delta L_{lim} = \frac{\lambda_0}{4\pi} \sqrt{\frac{hc \cdot \Delta f}{\eta P_0 \cdot \lambda_0}} \quad (11)$$

If the quantum efficiency of the detector $\eta = 0.3$, the source power $P_0 = 1$ mW, the source linewidth $\Delta f = 1$ kHz, $\lambda_0 = 1550$ nm, $h = 6.63 \times 10^{-34}$ m² kg/s, and $c = 3 \times 10^8$ m/s, we have $\Delta L_{lim} = 1.2 \times 10^{-3}$ nm. Such a small noise indicates that the shot noise is not the main factor to affect the system accuracy in the actual test.

The minimum detectable phase signal of the interferometer $\Delta\phi_{min det}$ is given by⁷

$$\Delta\phi_{min det} = \sqrt{(i_{shot}^2 + i_{elec}^2 + i_{RIN}^2)/(RI_0^2)} \quad (12)$$

where the circuit noise i_{elec} generally is 0.5 pA/ \sqrt{Hz} , the RIN (relative intensity) noise i_{RIN}^2 is 150 dB, i_{shot} is given by its definition.

As discussed above, the phase noise limit of the fiber interferometer with the fiber length of 1000 m should be considered as the comprehensive effect of the intrinsic thermal noise, source noise, shot noise and circuit noise. The phase noise is about $10^{-4} \sim 10^{-5}$ rad/Hz^{1/2}, and the measurement resolution of displacement is 1.2 pm ~ 12 pm/Hz^{1/2} according to Eq. (9).

The definition of the dynamic range is given by

$$DR = 20 \log L_{max}/L_{min} \quad (13)$$

Assume that the measurement range of the fiber seismometer is $\pm 1000 \mu\epsilon$, the arm length of the interferometer is 1000 m, then $L_{max} = 1$ m, and the range of the measurement resolution is $10^{-13} \sim 10^{-14} \epsilon$. Considering the temperature effect to the fiber seismometer, the range of the measurement resolution becomes $10^{-12} \sim 10^{-13} \epsilon$, and the dynamic range is higher than 200 dB.

3.3. The Elimination of Polarization Fading

The amplitude fading of the interference signal will take place when the polarization of two interference beams is not consistent, that is called polarization fading.⁹ One of the best methods to depress polarization fading is to using polarization-maintaining fiber in the sensing and reference arms. In addition adding a Faraday rotation mirror at the end of two interference arms of ordinary fiber, can also compensate the effect of signal polarization changes.¹⁰

3.4. The Noise Suppression of Light Frequency

Apart from the optical noises discussed above, the frequency noise of source is one of main noise source of fiber seismometer too. In practice, the light from the laser source have a certain linewidth δ_Δ , and it has a center frequency drift of $\Delta\nu$, as shown in Figure 2.

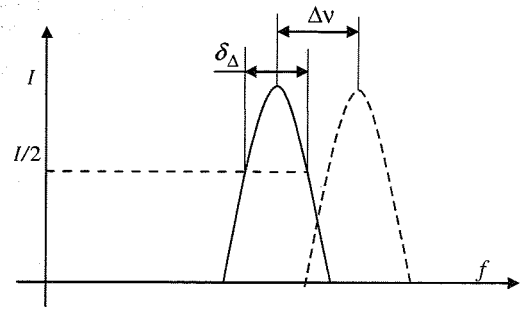


Fig. 2. Laser source phase noise.

The phase noise caused by the source frequency noise can be expressed as

$$\Delta\phi_{sf} = \frac{4\pi\Delta L}{c}(\delta_\Delta + \Delta\nu) \quad (14)$$

where ΔL is the arm length difference of the interferometer, c is the light velocity in vacuum.

According to the relationship between sensing phase and displacement, we can get:

$$\frac{L_{min}}{\Delta L} = \frac{\delta_\Delta}{\nu} + \frac{\Delta\nu}{\nu} \quad (15)$$

From Eq. (15), to reduce the source frequency noise caused phase noise, the length of the sensing arm should be approximately equal to that of the reference arm. In the present work, we employed the program of two sources: a narrow-linewidth single-frequency source for high precision detecting vibration signals, and a white-light source for matching the two interference arms.

According to the white-light interference theory, the intensity of the white-light interferometric signal can be given as¹¹

$$I(x) = \frac{1}{2} \alpha^2 n I_0 \left[1 + \exp\left(-\frac{\zeta^2}{2L_C^2} \cdot 4x^2\right) \cos\left(\frac{2\pi}{\lambda_0} \cdot 2x\right) \right] \quad (16)$$

where α is the insertion loss of a fiber coupler, n is the reflectivity of the arms, λ_0 is the central wavelength of source, ζ is the spectral coefficient, x is the optical path difference between the reference and sensing arms.

For the white-light source with $\lambda_0 = 1.31 \mu\text{m}$, $\Delta\lambda = 40$ nm, we can get its coherent length $L_C = 40 \mu\text{m}$. If the length difference between the arms is smaller than 1 mm, the phase noise caused by the frequency drift and linewidth of the source can be effectively reduced as long as the frequency stability $\Delta\nu/\nu$ is less than 10^{-8} and δ_Δ is lower than 1 MHz.

4. OPTICAL DESIGN OF THE FIBER SEISMOMETER

Based on the analysis above, the general design of a fiber seismometer is shown in Figure 3. The optical path of a fiber seismometer includes the following four parts:

(1) Light source system, consists of a 1550 nm narrow-linewidth DFB and a 1310 nm wide-spectrum SLD. Light

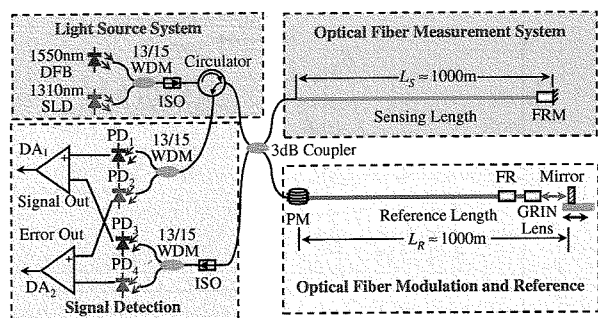


Fig. 3. Optical fiber seismic schematic.

emitted from the sources transmits through a 1310/1550 wavelength division multiplexer (WDM) and a fiber circulator, and then is divided into two beams by a 3 dB coupler. (2) Fiber measurement system, includes 1000 m long sensing fiber being wrapped around two concrete barriers, and a Faraday rotating mirror (FRM) at the end of the sensing fiber for eliminating the signal amplitude fading of the interference signal.

(3) Fiber reference modulation system, includes an optical modulator (PM), a reference fiber, a FRM, a fiber grin lens (GRIN) and an optical path matching system. Optical path matching system can make the optical paths of reference arm and sensing arm approximately equal (the difference of the optical path is about dozens of micron), which can greatly inhibit common-mode disturbance of two arms caused by temperature, reduce the demands on frequency stability of the light source, and improve the measurement accuracy.

(4) Signal detection system. The difference detection method is employed to receive the interference signals with the phase difference of 180° , which can eliminate the effect of DC drift, reduce noise, and improve the measurement accuracy of the interferometer. The interference arms are 1000 m, and they are wrapped 450 circles around a belt whose circumference is ~ 2.2 m. The sensing fiber is fixed on two concrete barriers with a distance of 2 m, and the reference arm is prevent from the vibration.

5. PRINCIPLE EXPERIMENT OF THE FIBER SEISMOMETER

We constructed a fiber seismometer prototype with fiber length of 1000 m, and measured its background noise of the seismometer without ground vibration interference, the seismometer was tested on a vibration isolation optical table. Frequency spectrum of the seismometer is shown in Figure 4, the peak at 30 Hz is a loaded vibration signal with an amplitude of 2 nm, and the peak at 50 Hz is electronic noise caused by power supply.

The relationship between the amplitude of frequency spectrum and radian is as follows:

$$A = 20 \lg \left(\frac{r}{2\sqrt{2}} \right) \quad (17)$$

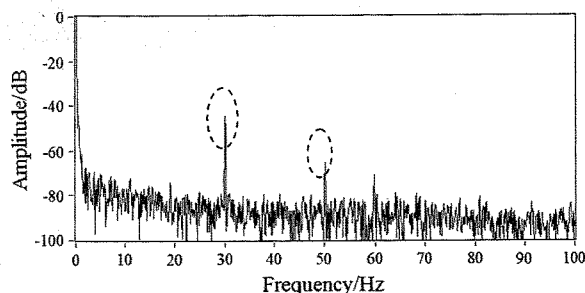


Fig. 4. Frequency spectrum of seismometer with 1000 m arm.

where A is amplitude in frequency spectrum, r is radian of corresponding signal. From Eq. (9), as wavelength of light source is 1550 nm, we can calculate that $1 \text{ rad} = 123.41 \text{ nm}$.

According to Eq. (17), the loaded signal with the amplitude of 2 nm would bring in a peak with -44.84 dB in frequency spectrum, which is consistent with the signal shown in Figure 4. Therefore, the resolution of the fiber seismometer prototype is better than $100 \text{ pm}/\sqrt{\text{Hz}}$.

6. CONCLUSION

In the paper, we present an Optical Fiber Seismometer with a Super-long Refraction Arm to detect weak crustal deformation and seismic information, study the parameter design of the optical path, comprehensively consider the effect of the intrinsic noise, such as thermal noise, Rayleigh noise and shot noise, optimize the sensitivity and resolution, analysis the principle of measurement and signal demodulation and establish the measurement transfer function.

Acknowledgments: This work was supported by the 973 program (No. 2010CB334701), the key project of Nature Science Foundation of Heilongjiang Province (No. ZD200810), the International Science and Technology Cooperation Program of China (Nos. 2010DFA22770, 2010DFR80140), and the special fund of central university basic scientific research (HEUCFZ1020) to Harbin Engineering University. In part supported by the National Natural Science Foundation of China (Nos. 61107069, 60927008, 61077062, 61177081 and 41174161).

References and Notes

1. M. Zumberge, J. Berger, J. Otero, and E. Wielandt, *Bulletin of the Seismological Society of America* 100, 598 (2010).
2. P. C. Leary, D. V. Manov, and Y. G. Li, *Bulletin of the Seismological Society of America* 80, 218 (1990).
3. H. L. Rivera, J. A. Garcia-Souto, and J. Sanz, *IEEE Journal of Selected Topics in Quantum Electronics* 6, 788 (2000).
4. A. Lebrun, B. Serio, M. Guilhem, P. Pfeiffer, S. Lecler, and A. Chakari, *Proceedings of SPIE-The International Society for Optical Engineering, Optical Sensing and Detection*, edited by F. Berghman, Brussels, BE (2010), Vol. 7726, p. 77262A-1.

5. Z. Gui-Cai, *The Principles and Technologies of Fiber-Optic Gyroscope*, edited by Z. Gui-Cai, National Defense Industry Press, Beijing (2008), Chap. 3, p. 70.
6. S. W. Lloyd, D. Vinayak, M. J. F. Digonnet, F. Shanhuai, and G. S. Kino, *Opt. Lett.* 35, 121 (2010).
7. C. K. Kirkendall and A. Dandridge, *J. Phys. D: Appl. Phys.* 37, R197 (2004).
8. K. H. Wanser, *Electron. Lett.* 28, 53 (1992).
9. L. Yan-Biao, *Polarization Optics*, edited by L. Peng, Science Press, Beijing (2003), Chap. 5, p. 158.
10. A. D. Kersey, M. J. Marrone, and M. A. Davis, *Electron. Lett.* 27, 518 (1991).
11. L. Tianchu, W. Anbo, M. Kent, and C. Richard, *Opt. Lett.* 20, 785 (1995).